Pergamon

Int. J. Solids Structures Vol. 32, No. 3/4, pp. 473–481, 1995

0020–7683/95 $9.50 + .00

0020–7683(94)00129–4

BIFURCATION IN ISOTROPIC THIN FILM/SUBSTRATE PLATES

N. J. SALAMON
Department of Engineering Science and Mechanics, 227 Hammond Building, The Pennsylvania State University, University Park, PA 16801, U.S.A.

and

CHRISTINE B. MASTERS
411 West Drive, Boalsburg, PA 16827, U.S.A.

(*Received* 23 *June* 1994)

Abstract—Formulae for the bifurcation of free–free, rectangular, isotropic, thin film/substrate plates under the action of intrinsic film stress and initial strain are developed. The formulae are in terms of fundamental material properties and plate parameters and are presented in a compact form. Bifurcation behavior over a range of material and geometric combinations, as well as limiting cases, are investigated.

INTRODUCTION

Bimaterial plate systems are prone to deflect under the influence of inelastic or initial stress and strain. The former occurs in the process of deposition of films onto substrates (Stoney, 1909); the films develop intrinsic stresses which alone are sufficient to cause deflection, but also accrue material properties different from the substrate, even when of the same material composition. The latter occurs under a temperature change in systems having a mismatch in properties (Timoshenko, 1925). Both phenomena may occur simultaneously. Under sufficiently high magnitudes of such stress or strain, bimaterial plates buckle. Mathematically their deflection fields bifurcate from a single solution into three solutions, two of which are stable.

A rectangular plate with free boundaries and composed of a thin film bonded to a substrate, such that both materials and the layered combination are at most orthotropic, has been studied by Masters and Salamon (1993, 1994), who employed approximate solutions of increasing order. An intrinsic stress σ^* in the film and initial strain ε^* in both layers, each field uniformly distributed and having equal orthogonal components acting in the plane, generate deflections in the plate, which is assumed to be held flat during application of these fields. For deflections which are large with respect to plate thickness, but small with respect to lateral plate dimensions, these approximations admit nonlinear total strains given by

$$\varepsilon_x = \varepsilon_x^0 - z\frac{\partial^2 w}{\partial x^2} \quad \varepsilon_y = \varepsilon_y^0 - z\frac{\partial^2 w}{\partial y^2} \quad \gamma_{xy} = \gamma_{xy}^0 - 2z\frac{\partial^2 w}{\partial x\,\partial y}, \tag{1}$$

where w is the plate deflection, x, y and z are Cartesian coordinates and

$$\varepsilon_x^0 = \frac{\partial u^0}{\partial x} + \frac{1}{2}\left(\frac{\partial w}{\partial x}\right)^2 \quad \varepsilon_y^0 = \frac{\partial v^0}{\partial y} + \frac{1}{2}\left(\frac{\partial w}{\partial y}\right)^2 \quad \gamma_{xy}^0 = \frac{\partial u^0}{\partial y} + \frac{\partial v^0}{\partial x} + \left(\frac{\partial w}{\partial x}\right)\left(\frac{\partial w}{\partial y}\right) \tag{2}$$

and where u^0 and v^0 are x- and y-directed midplane displacements.

Admissible fields, such that deflections, slopes and displacements vanish at the center, are prescribed as

$$u^0 = A_1 x + A_2 x^3 + A_3 x y^2 - a^2 x^3/6$$
$$v^0 = B_1 y + B_2 y^3 + B_3 x^2 y - b^2 y^3/6$$
$$w = (ax^2 + by^2)/2, \tag{3}$$

where A_i, B_i, a and b are unknown contants, but a and b denote constant curvature about the y and x axes, respectively, and are the object of the investigation.

The present paper is motivated by a need to know when bifurcation will occur in a thin-film system and to enable its calculation simply. Another purpose is to investigate bifurcation for different material combinations. To achieve tractability, the treatment is restricted to isotropic materials and to elastic strain fields composed of second degree polynomials, a lower order formulation given as case 3 in Masters and Salamon (1993) and case 2 in their sequel (1994). Importantly, this results in a more conservative estimate of bifurcation and can be achieved without the use of a computer. Further theoretical details and numerical results, as well as important references to supporting work, are presented there.

The approach is to minimize the strain energy density, which for each layer n is

$$U_n = \tfrac{1}{2}[\varepsilon_x^e\ \varepsilon_y^e\ \gamma_{xy}]\,[Q^n]\,[\varepsilon_x^e\ \varepsilon_y^e\ \gamma_{xy}]^T + [\sigma_x^*\ \sigma_y^*]\,[\varepsilon_x^e\ \varepsilon_y^e]^T, \tag{4}$$

where superscript e denotes elastic strains given by $\varepsilon_i^e = \varepsilon_i - \varepsilon_i^*$, $i = x$ and y, $[Q^n]$ is the matrix of elastic isotropic constants given in the Appendix, superscript T denotes the matrix transposed, and inelastic shear strain and intrinsic shear stress is taken as zero. Then, taking the first variation of the total potential energy of the plate, given by $\Sigma_n \int U_n \,dx\,dy\,dz$, with respect to the constants A_i, B_i, a and b, produces a system of equations in terms of bending curvatures a and b, which reduce to two expressions:

$$a = -\frac{H_1 b + H_2}{H_3 b^2 + H_4} \quad b = -\frac{H_1 a + H_2}{H_3 a^2 + H_4}, \tag{5}$$

where the H_i are composite material parameters and H_2 is also a function of intrinsic stress and initial strain. Specific formulae for these parameters are given in the Appendix.

The solutions for curvature are

$$a - b = 0 \quad ab = \text{constant}. \tag{6}$$

The first solution describes a spherical deflection shape (equal curvatures) which is stable prior to bifurcation; the second solution describes the stable transition through an ellipsoidal shape (unequal curvatures) to either of two cylindrical deflection shapes, the occurrence of either of which is equally likely after bifurcation.

The two corresponding solutions for intrinsic stress σ^* are

$$\sigma_s^* = [a(a^2 H_3 + H_4 + H_1) + H_2^\varepsilon]/H_2^\sigma \quad \sigma_e^* = [(a+b)H_4 + H_2^\varepsilon]/H_2^\sigma, \tag{7}$$

where subscripts s and e denote spherical and elliptical deformation states, respectively, H_2^σ is a composite material parameter and H_2^ε is a combination of composite material properties and initial strain, both given in the Appendix.

A plot of intrinsic stress vs curvature forms a typical pitchfork bifurcation alluded to in the opening paragraph and described above. Illustrations can be found in textbooks, for

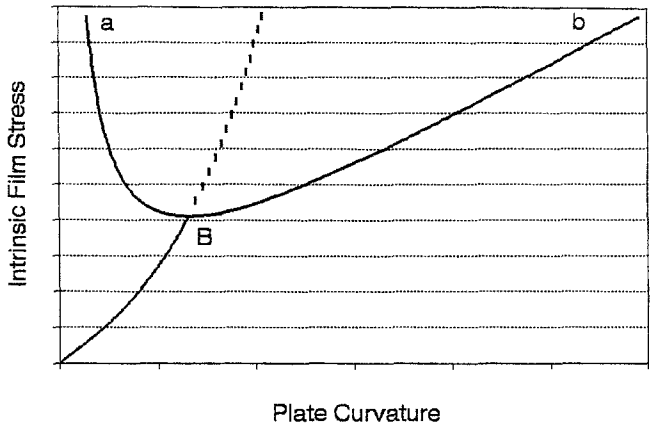

Fig. 1. Typical pitchfork bifurcation (dashed line unstable mode).

instance Brush and Almroth (1975). A typical example is shown in Fig. 1, where the dashed line denotes an unstable response. Plots of actual data can be found in the references.

The focus is solely upon bifurcation. After establishing relations for critical bifurcation curvature and intrinsic stress, they are transformed from composite plate parameters into fundamental material parameters. This leads to significant clarity and permits illustration of bifurcation behavior over a range of material stiffness ratios. Furthermore, special cases are then easily obtained.

BIFURCATION EQUATIONS

At the point of bifurcation, point B in Fig. 1, stresses and curvatures for the spherical and ellipsoidal deflected shapes coincide. Hence $\sigma_s^* = \sigma_e^* = \sigma_B^*$ and $a = b = \kappa_B$ where subscript B denotes a bifurcation value, σ_B is the intrinsic stress necessary to cause bifurcation and κ_B is the critical curvature for bifurcation, both of which occur at the limit of stable spherical curvature. Equating eqn (7) and substituting the latter into it leads to

$$\kappa_B = \pm\sqrt{(H_4 - H_1)/H_3}\,. \tag{8}$$

This expression permits calculation of the critical curvature for bifurcation purely in terms of material and geometric properties of the plate. It is independent of load, which also includes the initial strain parameter. Substitution of this result back into either of eqn (7) yields

$$\sigma_B^* = [2H_4(\pm\kappa_B) + H_2^\varepsilon]/H_2^\sigma, \tag{9}$$

where we deliberately insert $\pm$ to insure against sign errors between curvature and H_2^ε. Clearly one can invert eqn (9) to obtain curvature in terms of load, the more familiar form found in buckling theories, but independent of the side-lengths of the plate. In classical plate theory, if compressive forces are treated as intensities, force/length of side, an analogous result is obtained.

Equation (9) and its inverse can also be derived from solutions for ellipsoidal curvature given by Masters and Salamon (1993).

FUNDAMENTAL PARAMETERS

Let a flat plate with side dimensions X, Y be constructed by bonding a film to the lateral surface of a substrate, thicknesses t_f and t_s, respectively, to form a composite structure through the thickness. The film and substrate are isotropic materials with shear moduli and

Poisson's ratios G_f, ν_f and G_s, ν_s, respectively. Then the following dimensionless parameters are defined:

$$\Gamma = \frac{G_f}{G_s} \quad \upsilon_f = \frac{1+\nu_f}{1-\nu_f} \quad \upsilon_s = \frac{1+\nu_s}{1-\nu_s} \quad \rho = \frac{t_f}{t_s} \ll 1. \tag{10}$$

It may seem odd to employ shear moduli in a plate-bending problem, but in seeking compact expressions below, this adoption proved more efficient.

Because the intrinsic stress is assumed uniform through the thickness and the deformation mode is bending, for meaningful results, the film must be thin. Hence $\rho \ll 1$.

CURVATURE

The critical curvature for bifurcation is obtained by expanding eqn (8) in terms of fundamental material properties and substituting parameters given in eqn (10). If a geometric composite factor CF squared is first extracted, where

$$CF^2 = \frac{4[\Gamma\rho\upsilon_f+\upsilon_s]X^2Y^2+5[\Gamma\rho(\upsilon_f+1)+\upsilon_s+1](X^4+Y^4)}{2[\Gamma\rho\upsilon_f+\upsilon_s](\Gamma\rho+1)^2X^4Y^4}, \tag{11}$$

then the bifurcation curvature κ_B squared is found to be

$$\kappa_B^2 = 12t_s^2CF^2[(\Gamma\rho^2-1)^2+4\Gamma\rho(1+\rho)^2]. \tag{12}$$

Square plate

In the case of a square plate, $X = Y = L$, a nondimensional composite parameter γ given by

$$\gamma^2 = \frac{2[\Gamma\rho\upsilon_f+\upsilon_s]+5[\Gamma\rho(\upsilon_f+1)+\upsilon_s+1]}{[\Gamma\rho\upsilon_f+\upsilon_s](\Gamma\rho+1)^2} \tag{13}$$

is uncovered, hence the Greek notation. Then the curvature squared is found to be

$$\kappa_B^2|_L = 12\frac{t_s^2}{L^4}\gamma^2[(\Gamma\rho^2-1)^2+4\Gamma\rho(1+\rho)^2], \tag{14}$$

where the added notation is self evident and L is the side length of the plate.

This geometry being one of common interest is worth further investigation. In the above equations, the parameter product $\Gamma\rho$ appears in a natural way. Indeed in order-of-magnitude expansions, this product must be considered rather than each factor individually, because whereas $\rho \ll 1, \Gamma \gg 1$ is very possible. Hence it also is natural to choose it to study curvature over a range of material combinations. If a nondimensional curvature is defined as follows:

$$\hat{\kappa}_B|_L = \frac{L^2}{t_s}\sqrt{\frac{1+\nu_s}{24(6+\nu_s)}}\kappa_B \tag{15}$$

and plotted vs $\Gamma\rho$, it will be normalized to unity at $\Gamma\rho = 0$ (the reason will become clear subsequently).

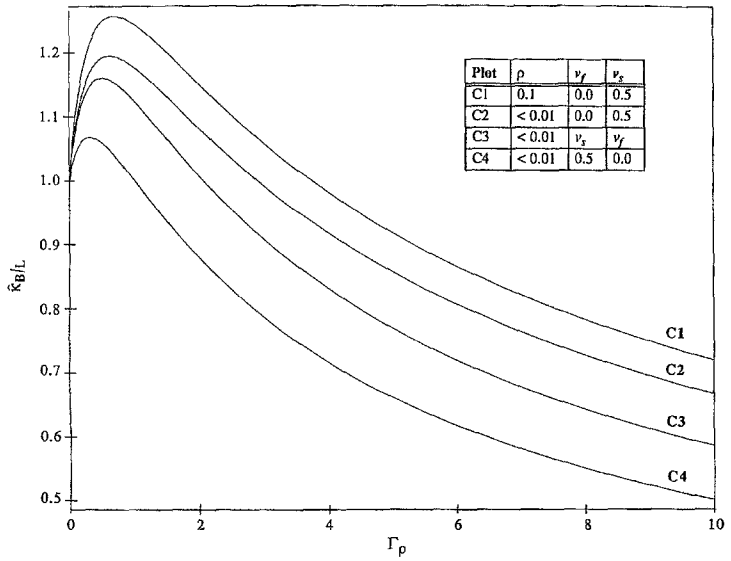

Fig. 2. Bifurcation curvature for a square plate.

Figure 2 illustrates the variation of nondimensional curvature given by eqn (15) over the range $0 \leqslant \Gamma\rho \leqslant 10$ and for the set of parameters listed in the table inset in the figure. Over this range, the selection is sufficient to see the extremes in behavior. The lowest and highest curves shown are very close to lower and upper bounds, respectively. For $\rho > 0.01$ and $(\upsilon_f, \upsilon_s) = (0, 0.5)$, the effect of ρ becomes pronounced, however magnitudes approaching 0.1 are probably stretching the assumption of small values; for $\rho < 0.01$, its effect on the lower curves is small, almost nil. When Poisson ratios are equal, the effect of ρ on the curves is nil (see below). For values of $\Gamma\rho < 1$ (the precise location of the peaks is rather cumbersome to evaluate), the bifurcation curvature increases with $\Gamma\rho$. Beyond the peaks, it decays very slowly. If ρ is held constant, then as Γ becomes large, associated with combinations of very stiff films on very compliant substrates, the curvature required to buckle the plate becomes very small, on the order of ρ^2. When $\Gamma\rho$, Γ and/or ρ vanishes, the curvature becomes

$$\kappa_B|_{L,\Gamma=0,\rho=0} = \frac{t_s}{L^2}\sqrt{\frac{24\,(6+\nu_s)}{1+\nu_s}}, \tag{16}$$

which explains the normalization above.

Equation (16) represents the case of a homogeneous plate with a uniform distribution of bidirectional initial shear stress on one lateral surface. It is difficult to relate this result to existing results for simply-supported plates under compressive loads because (1) the problems are different, and (2) the applied edge forces must be transformed into edge moments to obtain curvature, and this involves consideration of deflections and/or eccentricities in the position of the forces. Nevertheless the problems are similar. Referring to Brush and Almroth (1975) for instance, the curvature for Euler buckling of a square, simply supported plate under uniform, combined loading works out to be

$$\kappa_B|_{L,\mathrm{ref}} = \frac{\pi^2 t_s}{L^2}\left(\frac{1+c}{1+\nu}\right), \tag{17}$$

where c is a correction factor. These equations are only similar in form, but more is said below [eqn (25)].

Equal Poisson ratios

When the Poisson ratios are equal, $v_f = v_s = v$, and the geometries are rectangular, the composite factor becomes

$$CF^2|_v = \frac{2(1+v)X^2Y^2+5(X^4+Y^4)}{(1+v)(\Gamma\rho+1)^2X^4Y^4}, \tag{18}$$

where v is Poisson's ratio. This can be substituted directly into eqn (12) to obtain the curvature.

For a square plate,

$$\gamma^2|_v = \frac{2(6+v)}{(1+v)(\Gamma\rho+1)^2}, \tag{19}$$

which can be substituted into eqn (14) to obtain the curvature.

INTRINSIC STRESS

The intrinsic stress level necessary for bifurcation is obtained by expanding eqn (9) in terms of fundamental material properties and substituting parameters given in eqn (10). If the nondimensional parameter groups

$$\eta_1 = (\Gamma\rho v_f+v_s)(\Gamma\rho^3+1) \quad \eta_2 = (\Gamma\rho^2 v_f-v_s)^2$$
$$\eta_3 = \frac{\Gamma\rho(1+\rho)^2}{\Gamma\rho+1}[\Gamma\rho v_f(4v_s+3)+v_s(4v_f+3)] \tag{20}$$

are first extracted, then the intrinsic stress required for bifurcation is

$$\sigma_B^* = \frac{G_s t_s}{3\rho(1+\rho)v_s}(\eta_1+\eta_2+\eta_3)(\pm\kappa_B)+2G_s\Gamma v_f(\varepsilon_f^*-\varepsilon_s^*), \tag{21}$$

where the curvature is found from eqn (12), ε^* with subscripts f and s denotes initial strain in the film and substrate, respectively, and $\pm$ is again deliberately inserted to insure against sign errors in calculation. One observes that initial strain plays a very simple role in the generation of stress. Physically it is the mismatch in material properties that causes it. Hence if $\Gamma = 0$, initial strains have no effect.

Square plate

The intrinsic stress necessary for bifurcation of a square plate ($X = Y = L$) can be computed from eqn (21) by substituting the curvature from eqn (14) in place of that from eqn (12). Since the effect of the initial strains is evident, it will be ignored in illustrating the variation of intrinsic stress with system parameters. A nondimensional intrinsic stress necessary for bifurcation is defined as

$$\hat{\sigma}_B|_L = \frac{3L^2\rho(1+\rho)(1-v_s)}{4\sqrt{6}G_s t_s^2}\sqrt{\frac{1+v_s}{6+v_s}}\sigma_B^*|_L, \tag{22}$$

where $\sigma_B^*|_L$ is the intrinsic stress required to bifurcate a square plate, i.e. eqn (21), with curvature taken from eqn (14). When plotted against $\Gamma\rho$, eqn (22) will be normalized to unity at the origin (the scale factor will be made clear below).

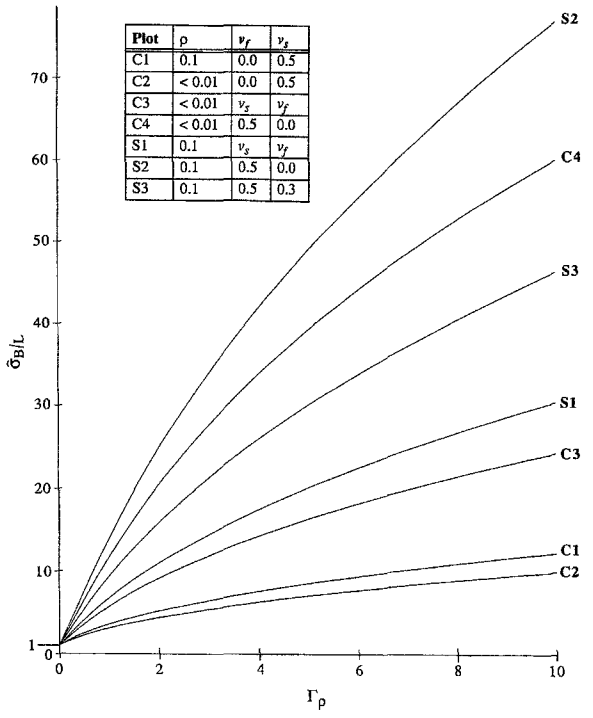

Fig. 3. Bifurcation stress for a square plate.

Figure 3 illustrates the variation of nondimensional intrinsic stress given by eqn (22) over the range $0 \leqslant \Gamma\rho \leqslant 10$ and for the set of parameters listed in the table inset in the figure. Over this range, the selection is sufficient to see the extremes in behavior. The lowest and highest curves shown are very close to lower and upper bounds, respectively. The intrinsic stresses are monotonically increasing with $\Gamma\rho$; for an infinite film-to-substrate stiffness ratio, the intrinsic stress necessary to bifurcate the plate is likewise infinite (recall that the bifurcation curvature only vanishes if ρ vanishes). Hence the factors $\Sigma\eta_i$ in eqn (21) overpower the bifurcation curvature. This is manifested in the order in which curves common to Figs 2 and 3 appear. The curves labeled C1 → C4 in Fig. 2 are ordered top to bottom from most to least compliant plates; those at the top reach larger critical curvatures to bifurcate. For the most part, ignoring small variations caused by ρ, in Fig. 3 the curves labeled C are reversed in order; the more compliant plates (lower curves) require less intrinsic stress for bifurcation. With increasing ρ, larger intrinsic stresses are required for bifurcation (compare S1, S2 with C3, C4), but the effect for $\rho \leqslant 0.01$ is nil.

When Γ vanishes, the intrinsic bifurcation stress becomes

$$\sigma_{\mathrm{B}}^{*}|_{L,\Gamma=0} = \frac{4\sqrt{6}G_{\mathrm{s}}t_{\mathrm{s}}^{2}}{3L^{2}\rho\,(1+\rho)\,(1-\nu_{\mathrm{s}})}\sqrt{\frac{6+\nu_{\mathrm{s}}}{1+\nu_{\mathrm{s}}}}, \tag{23}$$

which explains the scale factor in eqn (22). It is noted that the stress becomes infinite as $\rho \to 0$.

Equation (23) represents an initial stress uniformly distributed in a thin surface layer necessary to buckle a homogeneous plate. If one reverts to physical variables $\rho = t_{\mathrm{f}}/t_{\mathrm{s}}$ and lets $t_{\mathrm{f}} \to 0$ as $\sigma_{\mathrm{B}}^{*} \to \infty$ so that the product $t_{\mathrm{f}}\sigma_{\mathrm{B}}^{*} \to P_{\mathrm{B}}$, which is a shear force intensity in units of force/length of side, then on the one hand, the bidirectional force intensity, distributed over an infinitesimally thin surface layer, necessary to buckle a homogeneous plate becomes

$$P_{\mathrm{B}} = \lim_{\substack{t_{\mathrm{f}}\to 0 \\ \sigma_{\mathrm{B}}\to\infty}} t_{\mathrm{f}}\sigma_{\mathrm{B}}^{*} = \frac{2\sqrt{6}}{3}\sqrt{\frac{6+\nu_{\mathrm{s}}}{1+\nu_{\mathrm{s}}}}\frac{E_{\mathrm{s}}t_{\mathrm{s}}^{2}}{(1-\nu_{\mathrm{s}}^{2})L^{2}} = 1.633\sqrt{\frac{6+\nu_{\mathrm{s}}}{1+\nu_{\mathrm{s}}}}\frac{E_{\mathrm{s}}t_{\mathrm{s}}^{3}}{(1-\nu_{\mathrm{s}}^{2})L^{2}}, \tag{24}$$

where E_{s} is the modulus of elasticity for the substrate.

On the other hand, the Euler buckling load for a square, simply supported homogeneous plate under combined uniform compressive force intensity distributed around plate edges, Brush and Almroth (1975), is

$$P_B|_{ref} = 1.645\frac{E_s t_s^3}{(1-\nu_s^2)L^2}. \tag{25}$$

Interestingly the difference between eqns (24) and (25) is primarily the material factor $\sqrt{(6+\nu_s)/(1+\nu_s)}$. Again the difference between the two problems should be noted. Since eqn (24) determines a load distributed over a lateral plate surface, that is a load eccentrically positioned with respect to its middle surface, it fits into the class of problems for plates with imperfections. As such one would expect magnitudes of P_B generated by eqn (24) to be less than those from eqn (25), but they are not. However the loading in eqn (25) is a concentrated line load over the edges, hence magnitudes lower than eqn (24) would generate equal curvatures. So there is no contradiction. Comparison is further complicated by the different boundary conditions.

Equal Poisson ratios

When the Poisson ratios are equal, $\nu_f = \nu_s = \nu$, and the geometries rectangular, the intrinsic stress for bifurcation is

$$\sigma_B^*|_\nu = \frac{G_s t_s}{3\rho(1+\rho)}[(\Gamma\rho+1)(\Gamma\rho^3+1)+\upsilon(\Gamma\rho^2-1)^2 + \Gamma\rho(1+\rho)^2(4\upsilon+3)](\pm\kappa_B)|_\nu + 2G_s\Gamma\upsilon(\varepsilon_f^*-\varepsilon_s^*), \tag{26}$$

where eqns (12) and (18) are to be employed for the curvature.

For a square plate, eqn (26) also applies, but eqns (14) and (19) are to be employed for the curvature.

CONCLUSION

Formulae for the bifurcation of free–free, rectangular, isotropic, thin film/substrate plates under the action of intrinsic film stress and initial strain are developed. The formulae are in terms of fundamental material properties and plate parameters and are presented in a compact form. In the limit of a vanishing film thickness, the problem reduces to bifurcation of a homogeneous plate under a uniform distribution of bidirectional shear load intensity over one lateral surface; interestingly, these results are similar to classical results for buckling of homogeneous, simply supported plates under combined edge loading, even though the problems are different.

Limiting cases for square plates and equal Poisson ratios are studied in more detail. The product of the material stiffness ratio times the film-to-substrate thickness ratio, denoted $\Gamma\rho$, which appears naturally in the analysis, is the independent variable chosen for investigating different material combinations. When plotted against $\Gamma\rho$, it is found that the critical curvature at bifurcation rises to a peak value when the product is less than unity, then slowly decays to a small value as $\Gamma\rho$ approaches infinity. For a constant film thickness, this implies that when $\Gamma\rho$ is to the left of this peak, increasing the film stiffness increases the flexibility of the composite system, which is contrary to intuition; for $\Gamma\rho$ to the right of the peak, conservatively for $\Gamma\rho \geqslant 1$, increasing stiffness in films less compliant than the substrate increases stiffness of the system. It is noted that $\Gamma\rho < 1$ does not imply a more compliant film since $\rho < 1$, hence ρ must be considered in determining compliance ratios.

The intrinsic stress necessary for bifurcation rises monotonically with $\Gamma\rho$. Thus stiffening and/or thickening the film, for instance, increases the resistance to bifurcation.

A reduction in the elastic constants necessary to describe composite behavior similar to the Dundurs constants (Gerstner and Dundurs, 1969), which appear in plane and axisymmetric, infinite space problems were not discovered.

The formulae presented are compact and open to analysis. Their basis rests upon a reasonably accurate, but conservative theory for bifurcation.

Acknowledgement—The first author is grateful to Professor John Dundurs who taught him writing, thoroughness, professional integrity, as well as elasticity.

REFERENCES

Brush, D. O. and Almroth, B. O. (1975). *Buckling of Bars, Plates and Shells*. McGraw-Hill, New York.

Gerstner, R. W. and Dundurs, J. (1969). Representation of stress concentration factors for a composite in plane strain. *J. Compos. Mater.* **3,** 108–115.

Masters, C. B. and Salamon, N. J. (1993). Geometrically nonlinear stress–deflection relations for thin film/substrate systems. *Int. J. Engng. Sci.* **31,** 915–925.

Masters, C. B. and Salamon, N. J. (1994). Geometrically nonlinear stress–deflection relations for thin film/substrate systems with a finite element comparison. *ASME J. Appl. Mech.* In press.

Stoney, G. G. (1909). The tension of metallic films deposited by electolysis. *Proc. R. Soc. Lond. Ser. A* **82,** 172–175.

Timoshenko, S. (1925). Analysis of bi-metal thermostats. *J. Opt. Soc. Am.* **25,** 233–255.

APPENDIX

$$H_1 = D_{12}(A_{11}^2 - A_{12}^2) - 2A_{11}B_{11}B_{12} + A_{12}(B_{11}^2 + B_{12}^2)$$

$$H_2 = (A_{11} - A_{12})[(A_{11} + A_{12})(M_\varepsilon^* - M_\sigma^*) - (B_{11} + B_{12})(N_\varepsilon^* - N_\sigma^*)] = H_2^\varepsilon - H_2^\sigma \sigma^*$$

$$H_2^\varepsilon = (A_{11} - A_{12})[(A_{11} + A_{12})M_\varepsilon^* - (B_{11} + B_{12})N_\varepsilon^*]$$

$$H_2^\sigma = (A_{11} - A_{12})[(A_{11} + A_{12})t_f t_s/2 - (B_{11} + B_{12})t_f]$$

$$H_3 = (A_{11}^2 - A_{12}^2)^2 A_{33} L_x^4 L_y^4 / [144((A_{11}^2 - A_{12}^2)L_x^2 L_y^2 + 5A_{33}A_{11}(L_x^4 + L_y^4))]$$

$$H_4 = D_{11}(A_{11}^2 - A_{12}^2) + 2A_{12}B_{11}B_{12} - A_{11}(B_{11}^2 + B_{12}^2),$$

where

$$[A] = \int_{-h/2}^{h/2} [Q^n]\,\mathrm{d}z, \qquad [B] = \int_{-h/2}^{h/2} [Q^n] z\,\mathrm{d}z, \qquad [D] = \int_{-h/2}^{h/2} [Q^n] z^2\,\mathrm{d}z$$

$$\{N_\varepsilon^*\} = \int_{-h/2}^{h/2} [Q^n]\{\varepsilon^*\}\,\mathrm{d}z, \qquad \{N_\sigma^*\} = \int_{-h/2}^{h/2} \{\sigma^*\}\,\mathrm{d}z,$$

$$\{M_\varepsilon^*\} = \int_{-h/2}^{h/2} [Q^n]\{\varepsilon^*\} z\,\mathrm{d}z, \qquad \{M_\sigma^*\} = \int_{-h/2}^{h/2} \{\sigma^*\} z\,\mathrm{d}z,$$

and

$$Q_{11}^n = Q_{22}^n = \frac{2G_n}{1 - \nu_n}, \qquad Q_{12}^n = \nu_n Q_{11}^n$$

$$Q_{33}^n = G_n, \qquad Q_{13}^n = Q_{23}^n = 0.$$